BNL-99184-2013-TECH
C-A/AP/29;BNL-99184-2013-IR

RF Capture Simulation for Gold Ions in AGS

C. J. Gardner

October 2000

Collider Accelerator Department
Brookhaven National Laboratory

U.S. Department of Energy
USDOE Office of Science (SC)

DISCLAIMER

C-A/AP/#29
October 2000

RF Capture Simulation for Gold Ions in AGS

C.J. Gardner

Collider-Accelerator Department
Brookhaven National Laboratory
Upton, NY 11973

RF Capture Simulation for Gold Ions in AGS

C.J. Gardner

October 31, 2000

Under the present setup for RHIC operation, **four batches of six bunches** of gold ions (Au^{77+}) are injected into the AGS at constant magnetic field on the injection porch of **each AGS magnetic cycle**. The bunches are injected into stationary RF buckets at harmonic 24 with the RF voltage adjusted to match the buckets to the bunches as closely as possible. (Due to the large energy spread of the ions emerging from the stripping foil in the BTA line, the required voltage is close to the maximum available—some 320 kV.) Shortly after the four batches have been injected, the RF voltage is slowly reduced to zero, adiabatically debunching the beam. This is done because the 24 bunches need to be merged into 4 bunches to meet the luminosity requirements of RHIC. Debunching adiabatically prevents filamentation of the longitudinal emittance (i.e. preserves the "gross emittance") and reduces the energy spread of the beam.

Once debunched and while still on the injection porch, the beam is adiabatically rebunched at harmonic 4. This is done with a single RF cavity, the so-called KEK cavity, which is the only cavity that can operate at the required low frequency. The other AGS cavities operate at harmonic 12 and are used to accelerate the beam from injection to full energy. Once the beam has been bunched at harmonic 4, the amplitude of this harmonic is slowly decreased to zero and at the same time harmonic 8 is brought on (in the KEK cavity) with every other harmonic 8 bucket centered on a harmonic 4 bucket. As the harmonic 8 and 4 amplitudes are respectively increased and decreased adiabatically, the bunch widths are reduced and the four bunches are captured into every other harmonic 8 bucket. This makes it possible for each bunch to fit inside a harmonic 12 bucket when these are brought on. Finally, bringing on harmonic 12, one ends up with beam captured in every third of 12 stationary buckets on the injection porch.

This capture scheme was conceived by J. M. Brennan and was successfully implemented by the RF group for the FY2000 RHIC Run. In this note we examine the scheme by numerical simulation.

1 Turn-by-Turn Equations of Motion

Calculation of the evolution of a given particle distribution during capture into stationary buckets at constant magnetic field requires a suitable set of turn-by-turn equations for the longitudinal motion. These are derived here following the treatment of MacLachlan [1].

1.1 Synchronous Parameters

Let $2\pi R$ and ρ be the circumference and radius-of-curvature of the design orbit in a given ring, and let B and $2\pi R_s$ be the magnetic field and orbit circumference for the synchronous particle. We assume that B and R_s are given and calculate the other synchronous particle parameters in terms of these. Thus the radius-of-curvature is

$$\rho_s = \rho(R_s/R)^{1/\alpha}, \quad \alpha = \frac{1}{\gamma_t^2} \tag{1}$$

and the momentum and energy are

$$cp_s = eQB\rho_s, \quad E_s = \sqrt{(cp_s)^2 + m^2c^4}. \tag{2}$$

Here α is the "momentum compaction" factor, γ_t is the transition gamma, e is the proton charge, and eQ and m are the charge and mass of the particle. The synchronous β, γ and angular velocity are

$$\beta_s = cp_s/E_s, \quad \gamma_s = E_s/(mc^2), \quad \omega_s = c\beta_s/R_s. \tag{3}$$

We also define the phase slip factor

$$\eta_s = \alpha - \frac{1}{\gamma_s^2} = \frac{1}{\gamma_t^2} - \frac{1}{\gamma_s^2}. \tag{4}$$

1.2 Time Equation

We consider a ring with a single RF gap. Let T_n^s and T_n be respectively the times at which the synchronous and asynchronous particles make their

nth pass through the gap. The synchronous particle experiences no acceleration in the gap and revolves around the ring with constant angular velocity ω_s. Thus

$$T^s_{n+1} = T^s_n + T_s, \quad T_s = 2\pi/\omega_s, \tag{5}$$

and taking $T^s_1 = 0$, it follows that

$$T^s_{n+1} = nT_s. \tag{6}$$

Similarly, for the asynchronous particle we have

$$T_{n+1} = T_n + 2\pi/\omega_n \tag{7}$$

where ω_n is the angular velocity just after the nth pass through the gap. Defining

$$t_n = T_n - T^s_n, \quad t_{n+1} = T_{n+1} - T^s_{n+1} \tag{8}$$

we then have

$$t_{n+1} = t_n + 2\pi\left(\frac{1}{\omega_n} - \frac{1}{\omega_s}\right) = t_n + \left(\frac{\omega_s - \omega_n}{\omega_n}\right) T_s. \tag{9}$$

1.3 Energy Equation

Now let E_n be the energy of the asynchronous particle just after its nth pass through the gap. Then we have

$$E_{n+1} = E_n + eQV(T_{n+1}), \tag{10}$$

where $V(T)$ is the voltage across the the gap at time T. Since the synchronous particle undergoes no acceleration we must have

$$V(T^s_n) = 0 \tag{11}$$

for all n. We shall also assume that

$$V(T + T_s/h) = V(T) \tag{12}$$

where h, the harmonic number, is a positive integer. In terms of E_n, the other asynchronous parameters are

$$cp_n = \sqrt{E_n^2 - m^2c^4}, \quad \beta_n = cp_n/E_n \tag{13}$$

and

$$\rho_n = \frac{cp_n}{eQB}, \quad R_n = R(\rho_n/\rho)^\alpha, \quad \omega_n = c\beta_n/R_n. \tag{14}$$

Defining

$$e_n = E_n - E_s, \quad e_{n+1} = E_{n+1} - E_s \tag{15}$$

and using

$$T_{n+1} = t_{n+1} + T^s_{n+1} = t_{n+1} + nT_s \tag{16}$$

and

$$V(t_{n+1} + nT_s) = V(t_{n+1}), \tag{17}$$

we can write (10) as

$$e_{n+1} = e_n + eQV(t_{n+1}). \tag{18}$$

This, together with

$$t_{n+1} = t_n + \left(\frac{\omega_s - \omega_n}{\omega_n}\right) T_s \tag{19}$$

gives the turn-by-turn longitudinal motion of the asynchronous particle.

1.4 Sympletic Map

The Jacobian matrix elements for the map from $(t_n,\, e_n)$ to $(t_{n+1},\, e_{n+1})$ are

$$\frac{\partial t_{n+1}}{\partial t_n} = 1, \quad \frac{\partial t_{n+1}}{\partial e_n} = 2\pi \frac{\partial (1/\omega_n)}{\partial e_n} \tag{20}$$

$$\frac{\partial e_{n+1}}{\partial t_n} = eQV', \quad \frac{\partial e_{n+1}}{\partial e_n} = 1 + 2\pi eQV' \frac{\partial (1/\omega_n)}{\partial e_n} \tag{21}$$

where V' is the derivative of V with respect to T at time T_{n+1}. Thus we have

$$\left(\frac{\partial t_{n+1}}{\partial t_n}\right)\left(\frac{\partial e_{n+1}}{\partial e_n}\right) - \left(\frac{\partial t_{n+1}}{\partial e_n}\right)\left(\frac{\partial e_{n+1}}{\partial t_n}\right) = 1 \tag{22}$$

and the map is symplectic. If $t_n = 0$ and $e_n = 0$, then it follows from (18) and (19) that $t_{n+1} = 0$ and $e_{n+1} = 0$. Thus if $t_1 = 0$ and $e_1 = 0$ it follows by induction that $t_n = 0$ and $e_n = 0$ for all n, and we see that the point $(t_1,\, e_1) = (0,\, 0)$ is a fixed point.

1.5 Approximate Time Equation

Now

$$\frac{\omega_s}{\omega_n} = 1 - \left(\frac{\omega_n - \omega_s}{\omega_s}\right) + \left(\frac{\omega_n - \omega_s}{\omega_s}\right)^2 - \left(\frac{\omega_n - \omega_s}{\omega_s}\right)^3 + \cdots \tag{23}$$

and, to first order in $p_n - p_s$ and $E_n - E_s$,

$$\left(\frac{\omega_n - \omega_s}{\omega_s}\right) = -\eta_s \left(\frac{p_n - p_s}{p_s}\right) = -\eta_s \left(\frac{E_n - E_s}{\beta_s^2 E_s}\right). \tag{24}$$

Thus, to first order we have

$$\frac{\omega_s}{\omega_n} = 1 - \left(\frac{\omega_n - \omega_s}{\omega_s}\right) = 1 + \eta_s \left(\frac{E_n - E_s}{\beta_s^2 E_s}\right) = 1 + \left(\frac{\eta_s}{\beta_s^2 E_s}\right) e_n \tag{25}$$

and equation (19) becomes

$$t_{n+1} = t_n + T_s \left(\frac{\eta_s}{\beta_s^2 E_s}\right) e_n. \tag{26}$$

This, together with

$$e_{n+1} = e_n + eQV(t_{n+1}) \tag{27}$$

again produces a symplectic map from $(t_n,\, e_n)$ to $(t_{n+1},\, e_{n+1})$.

1.6 Phase Equation

Let us now introduce new variables

$$\phi_n = h\omega_s t_n, \quad W_n = \frac{e_n}{h\omega_s}. \tag{28}$$

Here ϕ_n is the phase that corresponds to time t_n, and W_n is defined so that the transformation from $(t_n,\, e_n)$ to $(\phi_n,\, W_n)$ is symplectic. In terms of these variables equations (26) and (27) become

$$\phi_{n+1} = \phi_n + T_s \left(\frac{h^2\omega_s^2\eta_s}{\beta_s^2 E_s}\right) W_n \tag{29}$$

and

$$W_{n+1} = W_n + T_s \left(\frac{eQ}{2\pi h}\right) V\left(\frac{\phi_{n+1}}{h\omega_s}\right). \tag{30}$$

Defining

$$a = \left(\frac{h^2\omega_s^2\eta_s}{\beta_s^2 E_s}\right) \tag{31}$$

and

$$F(\phi_{n+1}) = \left(\frac{eQ}{2\pi h}\right) V\left(\frac{\phi_{n+1}}{h\omega_s}\right) \tag{32}$$

we then have

$$\phi_{n+1} = \phi_n + aT_s W_n \tag{33}$$

and

$$W_{n+1} = W_n + T_s F(\phi_{n+1}). \tag{34}$$

These equations again generate a sympletic map. Note that since $V(0) = 0$ and $V(T + T_s/h) = V(T_s)$ we have

$$F(0) = 0, \quad F(\phi + 2\pi) = F(\phi). \tag{35}$$

Since we are interested in the momentum deviation $p_n - p_s$, it is useful to have an expression for this in terms of W_n. Using (24) and (28) we find

$$\left(\frac{p_n - p_s}{p_s}\right) = \left(\frac{E_n - E_s}{\beta_s^2 E_s}\right) = \left(\frac{h\omega_s}{\beta_s^2 E_s}\right) W_n. \tag{36}$$

2 Hamiltonian Equations of Motion

The turn-by-turn motion given by equations (33) and (34) can be approximated by the motion that follows from a Hamiltonian. The Hamiltonian in this case is

$$H(\phi, W) = \frac{1}{2} a W^2 + U(\phi) \tag{37}$$

and the equations of motion are

$$\dot{\phi} = \frac{d\phi}{dt} = \frac{\partial H}{\partial W} = aW, \tag{38}$$

$$\dot{W} = \frac{dW}{dt} = -\frac{\partial H}{\partial \phi} = -\frac{\partial U}{\partial \phi} = F(\phi). \tag{39}$$

First-order symplectic integration [2] of these equations over time T_s yields the symplectic map given by (33) and (34).

2.1 Constants of the Motion

If $U(\phi)$ has no explicit dependence on the time, then $H(\phi, W)$ is constant for the motion generated by equations (38) and (39). However, it is only approximately constant for the motion generated by (33) and (34). As

shown in Ref. [2], one can construct approximate constants order-by-order in T_s. This is done explicitly to order T_s^2 in the Appendix. Here one finds

$$H(\phi_{n+1}, W_{n+1}) = H(\phi_n, W_n) + O(T_s^2) \tag{40}$$

where $O(T_s^2)$ are terms of order T_s^2 and higher. Proceeding further, one finds

$$G(\phi_{n+1}, W_{n+1}) = G(\phi_n, W_n) + O(T_s^3) \tag{41}$$

where

$$G(\phi, W) = H(\phi, W) - \frac{1}{2}\, aT_s W F(\phi) \tag{42}$$

and $O(T_s^3)$ are terms of order T_s^3 and higher.

2.2 Stable and Unstable Fixed Points

The fixed points, $(\phi_f,\, W_f)$, of the motion satisfy the equations

$$0 = \frac{\partial H}{\partial \phi} = \frac{\partial U}{\partial \phi} = -F(\phi), \quad 0 = \frac{\partial H}{\partial W} = aW. \tag{43}$$

Thus

$$F(\phi_f) = 0, \quad W_f = 0. \tag{44}$$

To determine whether the motion near a fixed point is stable or unstable we must examine the second derivative of U with respect to ϕ. Let $U_{\phi\phi}$ be the value of the second derivative at the fixed point. Then, when $a < 0$ (below transition), the motion near the fixed point will be stable if $U_{\phi\phi} < 0$ and unstable if $U_{\phi\phi} > 0$. Similarly when $a > 0$ (above transition), the motion near the fixed point will be stable if $U_{\phi\phi} > 0$ and unstable if $U_{\phi\phi} < 0$.

2.3 The Separatrix

Let H_u be the value of H at an unstable fixed point: $\phi = \phi_u$, $W = 0$. Then

$$H_u = U(\phi_u) \tag{45}$$

and the equation

$$H(\phi, W) = H_u \tag{46}$$

defines the separatrix. Solving this equation for $W^2(\phi)$ we obtain

$$W^2(\phi) = \frac{2}{a}\left\{U(\phi_u) - U(\phi)\right\}. \tag{47}$$

We also have

$$\frac{dW^2}{d\phi} = -\frac{2}{a}\frac{\partial U}{\partial \phi}, \quad \frac{d^2W^2}{d^2\phi} = -\frac{2}{a}\frac{\partial^2 U}{\partial \phi^2} \tag{48}$$

from which it follows that $W^2(\phi)$ reaches at local maximum at each stable ϕ_f. The area around a stable fixed point and bounded by the separatrix is an RF bucket. The height, W_b, of the bucket is given by

$$W_b^2 = \frac{2}{a}\{U(\phi_u) - U(\phi_s)\} \tag{49}$$

where ϕ_s is the stable ϕ_f.

3 Capture Simulation

Let us now use equations of Sections 1 and 2 to simulate the capture process on the injection porch in the AGS.

3.1 AGS and Gold Parameters

Gold ions are injected into the AGS with $Q = 77$, $mc^2 = 183.434144$ GeV, and magnetic rigidity $B\rho_s = 3.721589$ Tm. We shall take

$$\rho_s = \rho = 85.387 \text{ meters}, \quad R_s = R = 4R_r/19, \quad \gamma_t = 8.5 \tag{50}$$

where $R_r = 3833.845/(2\pi)$ meters is the nominal RHIC radius. This gives $R = 4R_r/19 = 128.4580$ meters, which is approximately 5 mm larger than the nominal AGS radius reported by Bleser [3]. The momentum and energy of the synchronous gold ion are

$$cp_s = eQB\rho_s, \quad E_s = \sqrt{(cp_s)^2 + m^2c^4} \tag{51}$$

and β, γ and the angular velocity are

$$\beta_s = cp_s/E_s, \quad \gamma_s = E_s/(mc^2), \quad \omega_s = c\beta_s/R_s. \tag{52}$$

Putting in numbers we get $B = 435.894$ Gauss, $cp_s/n = 436.087$ MeV, $E_s/n = 1028.20$ MeV, $\beta_s = 0.424128$, $T_s = 2\pi/\omega_s = 6.34780$ μs, and $\gamma_s = 1.10424$. Here $n = 197$ is the number of nucleons in a gold nucleus. Since $\gamma_s < \gamma_t$, injection occurs below transition and we have $\eta_s < 0$ and $a < 0$.

3.2 Initial Particle Distribution

The initial particle distribution for the simulation is that of completely debunched beam. This is the situation on the injection porch after four batches of six bunches have been injected (into 24 stationary buckets) and debunched adiabatically. We assume a uniform distribution and consider an 80-by-80 array of points (particles) which cover the region

$$-\pi \le \phi \le \pi, \quad -W_I \le W \le W_I \tag{53}$$

occupied by one fourth of the beam. Here

$$W_I = E_I/(h\omega_s) = E_I T_s/(2\pi h) \tag{54}$$

where $2E_I$ is the energy width of the debunched beam and $h = 4$. The area of the region is

$$\epsilon = (2\pi)(2W_I) = 2E_I T_s/h = E_I T_s/2. \tag{55}$$

This is the total longitudinal emittance of 6 of the original 24 bunches. We shall take $\epsilon = 60$ eV-s which amounts to $60/197 = 0.305$ eV-s per nucleon. Each of the 6400 particles in the 80-by-80 array will be tracked using the turn-by-turn equations of Section 1. The equations of Section 2 give the parameters of the RF buckets which contain the particles.

3.3 Capture Program

For capture with harmonics 4, 8, and 12 on the AGS injection porch, we take 4 to be the fundamental harmonic, and 8 and 12 to be the second and third harmonics of the fundamental. Thus we put $h = 4$ in the turn-by-turn equations of Section 1 and we put

$$F(\phi) = A_1 \sin\phi + A_2 \sin 2\phi + A_3 \sin 3\phi \tag{56}$$

for $F(\phi)$ in the equations of Sections 1 and 2. Here

$$A_i = \left(\frac{eQV_i}{2\pi h}\right) \tag{57}$$

and V_1, V_2, V_3 are respectively the RF voltages for harmonics 4, 8, and 12. These are varied slowly (adiabatically) during the capture process.

3.3.1 Harmonic 4 Excitation

The capture process begins with the excitation of the KEK cavity at harmonic 4. A_2 and A_3 are zero and A_1 is brought up slowly from zero to A_K over time T_1. For $0 \le T \le T_1$, we have

$$F(\phi) = A_1 \sin\phi, \quad U(\phi) = A_1 \cos\phi \tag{58}$$

where

$$A_1(T) = A_K (T/T_1)^2. \tag{59}$$

Here the amplitude increases quadratically with time as is done in practice [4]. The unstable phases for the bucket centered on $\phi = 0$ are $\phi = \pm\pi$, and the bucket separatrix is given by

$$W^2(\phi) = \frac{2}{a}\left\{U(\pi) - U(\phi)\right\} = -\frac{2A_1}{a}\left\{1 + \cos\phi\right\}. \tag{60}$$

Using the identity $1 + \cos\phi = 2\cos^2(\phi/2)$, this becomes

$$W^2(\phi) = -\frac{4A_1}{a}\cos^2(\phi/2). \tag{61}$$

The bucket height, W_1, is given by

$$W_1^2 = \frac{2}{a}\left\{U(\pi) - U(0)\right\} = -\frac{4A_1}{a} = \left(\frac{-2eQV_1\beta_s^2 E_s}{\pi h^3 \omega_s^2 \eta_s}\right) \tag{62}$$

and the (single) bucket area is

$$B_1 = 2\int_{-\pi}^{\pi} W(\phi)\, d\phi = 2W_1 \int_{-\pi}^{\pi} \cos(\phi/2)\, d\phi = 8W_1. \tag{63}$$

Equating the unbunched beam emittance ($\epsilon = 60$ eV-s) with B_1, and solving for V_1, we obtain the minimum voltage required to capture the beam. Thus

$$\epsilon^2 = B_1^2 = 64W_1^2 = \left(\frac{-128eQV_1\beta_s^2 E_s}{\pi h^3 \omega_s^2 \eta_s}\right) \tag{64}$$

and

$$eV_1 = \left(\frac{-\epsilon^2 \pi h^3 \omega_s^2 \eta_s}{128 Q \beta_s^2 E_s}\right) = 1.6 \text{ keV}. \tag{65}$$

Of course, the actual voltage used will be much larger so that the captured beam ends up occupying the central region of a much larger bucket. The maximum voltage available in the KEK cavity is $V_K = 20$ kV. Setting $V_1 = V_K$ gives a maximum harmonic 4 bucket area $B_1 = 213$ eV-s (which amounts to $213/197 = 1.08$ eV-s per nucleon).

3.3.2 Harmonic 4 and 8 Excitation

Capture continues with KEK cavity excitation at both harmonics 4 and 8. A_1 is slowly reduced to zero as A_2 is slowly increased from zero to A_K over time $T_2 - T_1$. For $T_1 \le T \le T_2$, we have

$$F(\phi) = A_1 \sin\phi + A_2 \sin 2\phi = \{A_1 + 2A_2 \cos\phi\} \sin\phi, \tag{66}$$

and

$$U(\phi) = A_1 \cos\phi + \frac{1}{2} A_2 \{\cos 2\phi + 1\} = A_1 \cos\phi + A_2 \cos^2\phi \tag{67}$$

where

$$A_1(T) = A_K \left(\frac{T_2 - T}{T_2 - T_1}\right), \quad A_2(T) = A_K \left(\frac{T - T_1}{T_2 - T_1}\right). \tag{68}$$

Here the harmonic 4 amplitude decreases linearly from A_K at time T_1 to zero at time T_2. Similarly, the harmonic 8 amplitude increases linearly from zero at time T_1 to A_K at time T_2. This is approximately what is done in practice [4]. Initially, $2A_2 < A_1$ and the unstable phases for the bucket centered on $\phi = 0$ are $\phi_u = \pm\pi$. However, as soon as $2A_2$ becomes greater than A_1, these phases become stable and the unstable ones are given by

$$A_1 + 2A_2 \cos\phi_u = 0. \tag{69}$$

These move toward $\phi_u = \pm\pi/2$ as A_1 goes to zero. At time T_2, we have $A_1 = 0$, $A_2 = A_K$, and only harmonic 8 is excited. The bucket separatrix is then given by

$$W^2(\phi) = \frac{2}{a} \{U(\pi/2) - U(\phi)\} = -\frac{2A_2}{a} \cos^2\phi \tag{70}$$

and the bucket height, W_2, is given by

$$W_2^2 = \frac{2}{a} \{U(\pi/2) - U(0)\} = -\frac{2A_2}{a} = \left(\frac{-eQV_2\beta_s^2 E_s}{\pi h^3 \omega_s^2 \eta_s}\right). \tag{71}$$

Thus we can write

$$W^2(\phi) = W_2^2 \cos^2\phi \tag{72}$$

and the (single) bucket area is

$$B_2 = 2\int_{-\pi/2}^{\pi/2} W(\phi)\, d\phi = 2W_2 \int_{-\pi/2}^{\pi/2} \cos\phi\, d\phi = 4W_2. \tag{73}$$

Setting $V_2 = V_K = 20$ kV gives $B_2 = 75$ eV-s, the largest harmonic 8 bucket area available with the KEK cavity; this is not much larger than the 60 eV-s emittance we have assumed.

3.3.3 Harmonic 8 and 12 Excitation

Once the beam has been captured into every other bucket at harmonic 8, capture into every third bucket at harmonic 12 begins. A_2 is slowly reduced to zero as A_3 is slowly increased from zero to A over time $T_3 - T_2$. For $T_2 \le T \le T_3$, we have

$$\begin{aligned} F(\phi) &= A_2 \sin 2\phi + A_3 \sin 3\phi \\ &= 2A_2 \cos\phi \sin\phi + A_3 \left\{ 3\sin\phi - 4\sin^3\phi \right\} \\ &= \left\{ 2A_2 \cos\phi + A_3(4\cos^2\phi - 1) \right\} \sin\phi \end{aligned} \tag{74}$$

and

$$\begin{aligned} U(\phi) &= \frac{1}{2}A_2 \left\{ \cos 2\phi + 1 \right\} + \frac{1}{3}A_3 \cos 3\phi \\ &= A_2 \cos^2\phi + \frac{1}{3}A_3 \left\{ 4\cos^3\phi - 3\cos\phi \right\} \end{aligned} \tag{75}$$

where

$$A_2(T) = A_K \left(\frac{T_3 - T}{T_3 - T_2} \right), \quad A_3(T) = A \left(\frac{T - T_2}{T_3 - T_2} \right). \tag{76}$$

Here the harmonic 8 amplitude decreases linearly from A_K at time T_2 to zero at time T_3. Similarly, the harmonic 12 amplitude increases linearly from zero at time T_2 to A at time T_3. This, again, is approximately what is done in practice [4]. Solving

$$2A_2 \cos\phi + A_3(4\cos^2\phi - 1) = 0 \tag{77}$$

we find that for $A_3 > 0$, the unstable phases closest to $\phi = 0$ are given by

$$\cos\phi_u = \frac{-A_2 + \sqrt{A_2^2 + 4A_3^2}}{4A_3}, \tag{78}$$

and for $A_3 > 2A_2/3$, the stable phases closest to $\phi = 0$ are given by

$$\cos\phi_s = \frac{-A_2 - \sqrt{A_2^2 + 4A_3^2}}{4A_3}. \tag{79}$$

Thus, as A_2 goes to zero, the unstable phases move from $\pm\pi/2$ to $\pm\pi/3$, and, as soon as $A_3 > 2A_2/3$, the stable phases begin to move from $\pm\pi$ to

$\pm 2\pi/3$. At time T_3, we have $A_2 = 0$, $A_3 = A$, and only harmonic 12 is excited. The bucket separatrix is then given by

$$W^2(\phi) = \frac{2}{a}\left\{U(\pi/3) - U(\phi)\right\} = -\frac{2A_3}{3a}\left\{1 + \cos 3\phi\right\} \tag{80}$$

and the bucket height, W_3, is given by

$$W_3^2 = \frac{2}{a}\left\{U(\pi/3) - U(0)\right\} = -\frac{4A_3}{3a} = \left(\frac{-2eQV_3\beta_s^2 E_s}{3\pi h^3 \omega_s^2 \eta_s}\right). \tag{81}$$

Thus we can write

$$W^2(\psi/3) = \frac{1}{2}W_3^2\left\{1 + \cos\psi\right\} = W_3^2\cos^2(\psi/2) \tag{82}$$

and the (single) bucket area is

$$B_3 = 2\int_{-\pi/3}^{\pi/3} W(\phi)\, d\phi = \frac{2}{3}\int_{-\pi}^{\pi} W(\psi/3)\, d\psi = \frac{8W_3}{3}. \tag{83}$$

Setting $B_3 = \epsilon = 60$ eV-s and solving (81) for V_3, we find

$$eV_3 = \left(\frac{-27\epsilon^2\pi h^3\omega_s^2\eta_s}{128Q\beta_s^2 E_s}\right) = 43 \text{ keV}. \tag{84}$$

This is the minimum harmonic 12 voltage required to contain the 60 eV-s emittance we have assumed.

4 Results

The simulation was run with $T_1 = 100$ ms, $T_2 = 150$ ms, $T_3 = 200$ ms, and with

$$A_K = \left(\frac{eQV_K}{2\pi h}\right), \quad A = \left(\frac{eQV_A}{2\pi h}\right) \tag{85}$$

where $V_K = 20$ kV and $V_A = 60$ kV.

1. Figure 1 shows the beam distribution in the harmonic 4 bucket at time T_1. Here the rectangle outlines the region of the initial 60 eV-s uniform distribution. The harmonic 4 voltage at time T_1 is $V_1 = V_K = 20$ kV which gives bucket area $B_1 = 213$ eV-s. This is the largest harmonic 4 bucket area available.

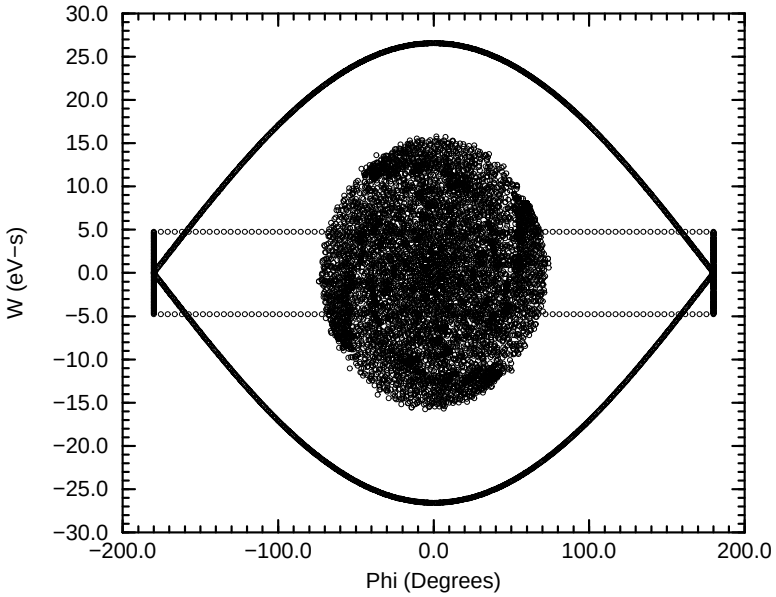

Figure 1: Capture into Harmonic 4 Bucket

2. Figure 2 shows the beam distribution in the harmonic 8 bucket at time T_2. (The original harmonic 4 bucket at time T_1 is also shown.) Here the harmonic 8 voltage is $V_2 = V_K = 20$ kV which gives bucket area $B_2 = 75$ eV-s. This is the largest harmonic 8 bucket area available and is barely large enough to contain the 60 eV-s beam emittance.

3. Figure 3 shows the beam distribution in the harmonic 12 bucket at time T_3. Here the harmonic 12 voltage is $V_3 = V_A = 60$ kV which gives bucket area $B_3 = 71$ eV-s. The bucket height is equal to that of the original harmonic 4 bucket. Although the bucket is large enough to contain the 60 eV-s emittance, a few particles have managed to leak into the adjacent buckets.

4. Figures 4, 5, 6 show the momentum distributions in the harmonic 4, 8, 12 buckets at times T_1, T_2, T_3 respectively. Here the time and fractional momentum deviation dp/p_s are given by equations (28) and (36).

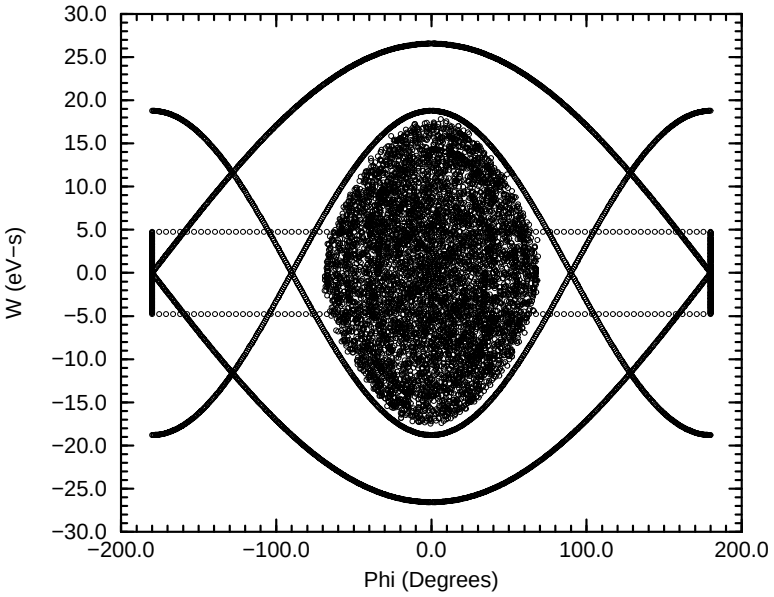

Figure 2: Capture into Harmonic 8 Bucket

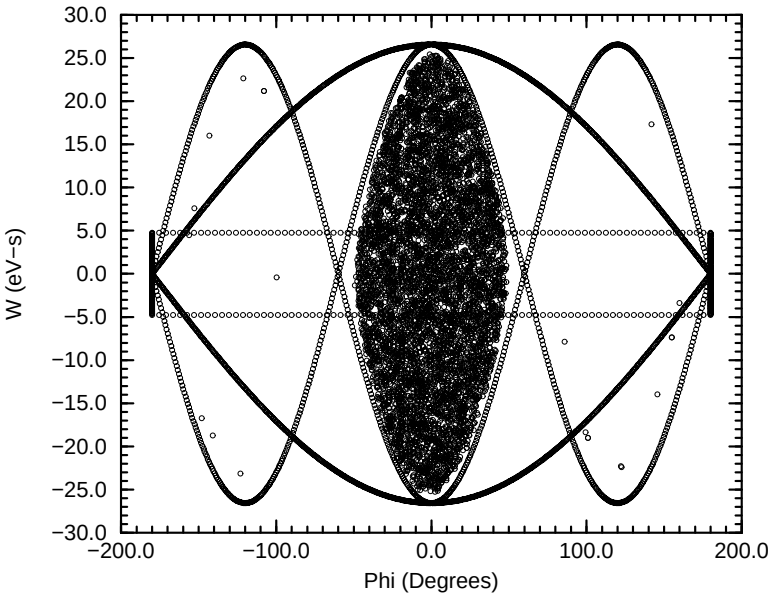

Figure 3: Capture into Harmonic 12 Bucket

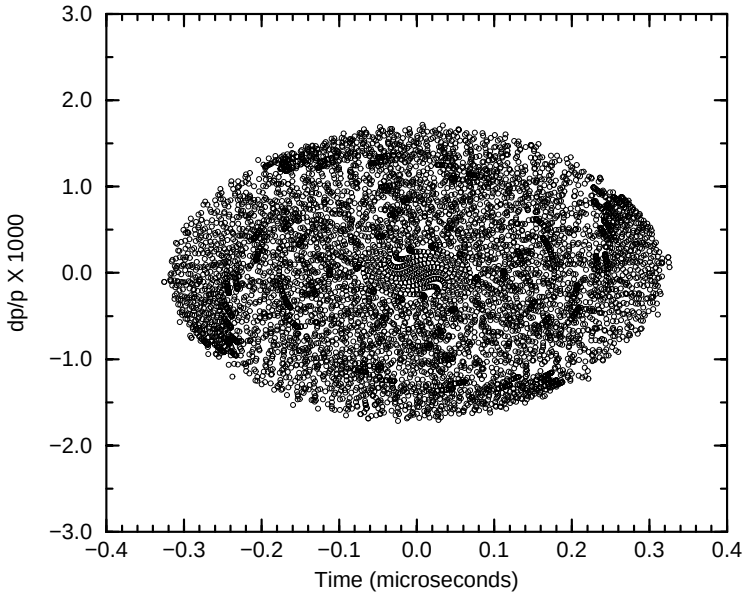

Figure 4: Momentum Distribution in Harmonic 4 Bucket

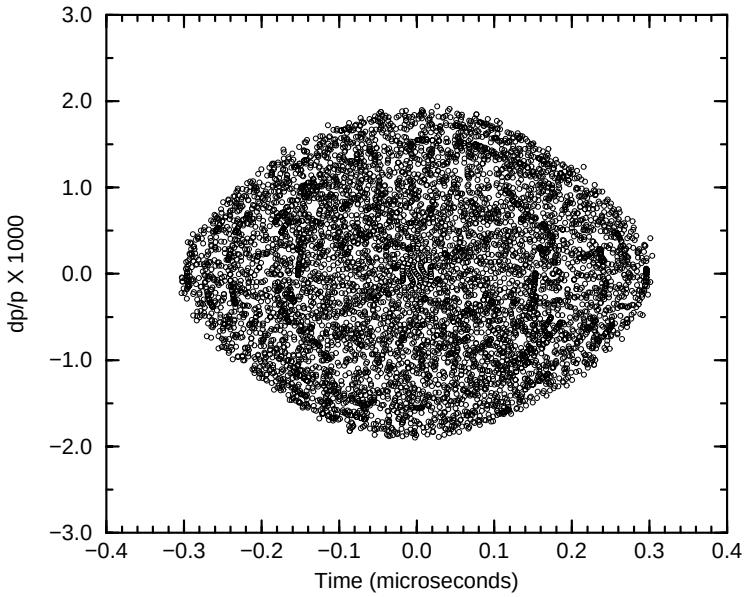

Figure 5: Momentum Distribution in Harmonic 8 Bucket

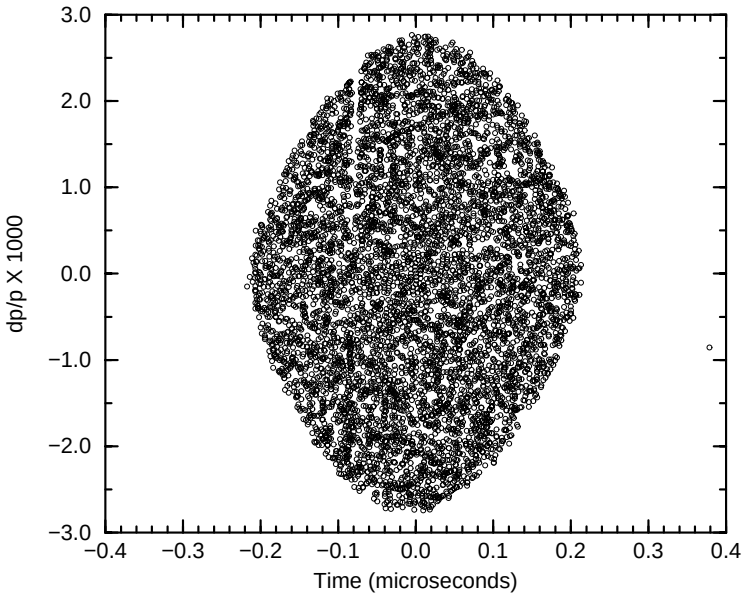

Figure 6: Momentum Distribution in Harmonic 12 Bucket

The "bottleneck" in the capture process is the harmonic 8 bucket area. Because this area is barely large enough to contain the 60 eV-s emittance, some particles can end up close to the unstable fixed points as the harmonic 8 voltage is decreased and the harmonic 12 voltage is increased. These presumably are the particles that have leaked into the adjacent harmonic 12 buckets in Figure 3. Increasing the maximum harmonic 12 voltage V_A from 60 to 120 kV and increasing the capture time T_3 from 200 to 250 ms, all but eliminates this leakage.

The simulation was also run with shorter capture times. With $T_1 = 50$ ms, $T_2 = 65$ ms, and $T_3 = 80$ ms, one sees a little more leakage into the adjacent harmonic 12 buckets as shown in Figure 7. These capture times are comparable to those used in practice [4].

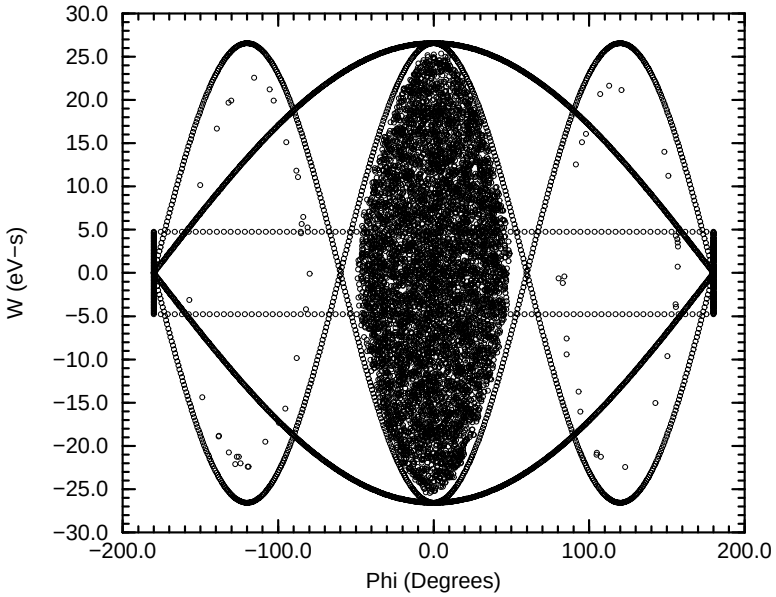

Figure 7: Harmonic 12 Buckets with Shorter Capture Time

5 Appendix

Consider the general Hamiltonian

$$H(\phi, W) = T(W) + U(\phi). \tag{86}$$

We then have the equations of motion

$$\frac{d\phi}{dt} = \frac{\partial H}{\partial W} = \frac{dT}{dW} = T' = g(W), \tag{87}$$

$$\frac{dW}{dt} = -\frac{\partial H}{\partial \phi} = -\frac{dU}{d\phi} = -U' = f(\phi). \tag{88}$$

The motion may be approximated by the symplectic map

$$\phi_1 = \phi + \tau g(W), \quad W_1 = W + \tau f(\phi_1). \tag{89}$$

We wish to find an approximate constant of the motion generated by this map. This can be done order-by-order in τ as discussed in Ref. [2]. Let

$$G(\phi, W) = H_0(\phi, W) + \tau H_1(\phi, W) \tag{90}$$

where H_0 and H_1 are functions to be determined. To first order in τ we have

$$H_0(\phi_1, W_1) = H_0(\phi, W) + \tau g(W)\frac{\partial H_0}{\partial \phi} + \tau f(\phi)\frac{\partial H_0}{\partial W}, \tag{91}$$

$$\tau H_1(\phi_1, W_1) = \tau H_1(\phi, W), \tag{92}$$

and

$$G(\phi_1, W_1) = G(\phi, W) + \tau g(W)\frac{\partial H_0}{\partial \phi} + \tau f(\phi)\frac{\partial H_0}{\partial W}. \tag{93}$$

If we choose H_0 such that

$$\frac{\partial H_0}{\partial \phi} = -f(\phi), \quad \frac{\partial H_0}{\partial W} = g(W) \tag{94}$$

then we will have

$$G(\phi_1, W_1) = G(\phi, W) \tag{95}$$

to first order in τ. Thus we take

$$H_0 = T(W) + U(\phi) = H. \tag{96}$$

Let us now calculate $G(\phi_1, W_1)$ to second order in τ. We have

$$G(\phi_1, W_1) = T(W_1) + U(\phi_1) + \tau H_1(\phi_1, W_1) \tag{97}$$

where

$$T(W_1) = T(W) + T'(W)(W_1 - W) + \frac{1}{2}T''(W_1 - W)^2, \tag{98}$$

$$U(\phi_1) = U(\phi) + U'(\phi)(\phi_1 - \phi) + \frac{1}{2}U''(\phi_1 - \phi)^2, \tag{99}$$

$$T' = g(W), \quad T''(W) = g'(W), \quad U' = -f(\phi), \quad U''(\phi) = -f'(\phi) \tag{100}$$

and

$$\tau H_1(\phi_1, W_1) = \tau H_1(\phi, W) + \tau(\phi_1 - \phi)\frac{\partial H_1}{\partial \phi} + \tau(W_1 - W)\frac{\partial H_1}{\partial W}. \tag{101}$$

Now

$$W_1 - W = \tau f(\phi_1), \quad \phi_1 - \phi = \tau g(W) \tag{102}$$

where

$$f(\phi_1) = f(\phi) + f'(\phi)(\phi_1 - \phi) = f(\phi) + f'(\phi)\tau g(W). \tag{103}$$

Thus, to second order in τ, we have

$$W_1 - W = \tau f(\phi) + \tau^2 f'(\phi) g(W) \tag{104}$$

$$(W_1 - W)^2 = \tau^2 f^2(\phi), \quad (\phi_1 - \phi)^2 = \tau^2 g^2(W). \tag{105}$$

Collecting terms we have

$$T(W_1) = T(W) + g(W)\{\tau f(\phi) + \tau^2 f'(\phi) g(W)\} + \frac{1}{2} g'(W)\tau^2 f^2(\phi), \tag{106}$$

$$U(\phi_1) = U(\phi) - f(\phi)\tau g(W) - \frac{1}{2} f'(\phi)\tau^2 g^2(W), \tag{107}$$

and

$$T(W_1) + U(\phi_1) = T(W) + U(\phi) + \frac{1}{2}\tau^2 f'(\phi) g^2(W) + \frac{1}{2}\tau^2 g'(W) f^2(\phi). \tag{108}$$

We also have

$$\tau H_1(\phi_1, W_1) = \tau H_1(\phi, W) + \tau^2 g(W)\frac{\partial H_1}{\partial \phi} + \tau^2 f(\phi)\frac{\partial H_1}{\partial W}. \tag{109}$$

Using (108) and (109) in (97), we then have

$$\begin{aligned} G(\phi_1, W_1) &= G(\phi, W) + \frac{1}{2}\tau^2 f'(\phi) g^2(W) + \frac{1}{2}\tau^2 g'(W) f^2(\phi) \\ &+ \tau^2 g(W)\frac{\partial H_1}{\partial \phi} + \tau^2 f(\phi)\frac{\partial H_1}{\partial W}. \end{aligned} \tag{110}$$

Thus, choosing H_1 such that

$$\frac{\partial H_1}{\partial \phi} = -\frac{1}{2} f'(\phi) g(W), \quad \frac{\partial H_1}{\partial W} = -\frac{1}{2} f(\phi) g'(W) \tag{111}$$

we see that $G(\phi_1, W_1) = G(\phi, W)$ to second order in τ. Taking

$$H_1 = -\frac{1}{2} f(\phi) g(W) \tag{112}$$

gives the desired result.

References

[1] J.A. MacLachlan, "Difference Equations for Longitudinal Motion in a Synchrotron", Fermilab internal report FNAL FN-529, December 15, 1989; "Differential Equations for Longitudinal Motion in a Synchrotron", Fermilab internal report FNAL FN-532, January 25, 1990.

[2] H. Yoshida, Numerical Integration Methods, Handbook of Accelerator Physics and Engineering, Edited by A.W. Chao and M. Tigner, World Scientific, 1999, pp. 85–87.

[3] E.J. Bleser, "Where are the AGS Magnets", Accelerator Division Technical Note 215, May 20, 1985.

[4] As set up and documented by K.S. Smith.